

Holocene Carbon Stocks and Carbon Accumulation Rates Altered in Soils Undergoing Permafrost Thaw

Caitlin E. Hicks Pries,* Edward A. G. Schuur, and K. Grace Crummer

Department of Biology, University of Florida, 220 Bartram Hall, Gainesville, Florida 32611, USA

ABSTRACT

Permafrost soils are a significant global store of carbon (C) with the potential to become a large C source to the atmosphere. Climate change is causing permafrost to thaw, which can affect primary production and decomposition, therefore affecting ecosystem C balance. To understand future responses of permafrost soils to climate change, we inventoried current soil C stocks, investigated $\Delta^{14}\text{C}$, C:N, $\delta^{13}\text{C}$, and $\delta^{15}\text{N}$ depth profiles, modeled soil C accumulation rates, and calculated decadal net ecosystem production (NEP) in subarctic tundra soils undergoing minimal, moderate, and extensive permafrost thaw near Eight Mile Lake (EML) in Healy, Alaska. We modeled decadal and millennial soil C inputs, decomposition constants, and C accumulation rates by plotting cumulative C inventories against C ages based on radiocarbon dating of surface and deep soils, respectively. Soil C stocks at EML were substantial, over 50 kg C m^{-2} in the top meter, and did not differ much among sites. Carbon to nitrogen ratio, $\delta^{13}\text{C}$, and $\delta^{15}\text{N}$

depth profiles indicated most of the decomposition occurred within the organic soil horizon and practically ceased in deeper, frozen horizons. The average C accumulation rate for EML surface soils was $25.8 \text{ g C m}^{-2} \text{ y}^{-1}$ and the rate for the deep soil accumulation was $2.3 \text{ g C m}^{-2} \text{ y}^{-1}$, indicating these systems have been C sinks throughout the Holocene. Decadal net ecosystem production averaged $14.4 \text{ g C m}^{-2} \text{ y}^{-1}$. However, the shape of decadal C accumulation curves, combined with recent annual NEP measurements, indicates soil C accumulation has halted and the ecosystem may be becoming a C source. Thus, the net impact of climate warming on tundra ecosystem C balance includes not only becoming a C source but also the loss of C uptake capacity these systems have provided over the past ten thousand years.

Key words: permafrost thaw; carbon accumulation; net ecosystem production; radiocarbon; soil carbon inventory; carbon pools; tundra.

INTRODUCTION

One of the most significant global stores of carbon (C) lies within the soils of the northern hemisphere's permafrost zone. In this zone, an estimated 1672 Pg

C is stored—twice the current atmospheric C pool (Tarnocai and others 2009). Eighty-eight percent of this C is frozen within actual permafrost (Tarnocai and others 2009). Over hundreds to thousands of years, permafrost has protected organic C from microbial degradation and allowed C to accumulate in soils. This vast store of C is now vulnerable due to accelerated warming at high latitudes (IPCC 2007). Permafrost area is projected to decrease substantially by 2100 with twenty (Schaefer and others 2011) to eighty-nine (Lawrence and others

Received 4 July 2011; accepted 7 October 2011

Author contributions: CEHP helped design study, performed research, analyzed the data, and wrote the paper; EAGS conceived of study and contributed to writing the paper; and KGC performed research.

*Corresponding author; e-mail: chicks@ufl.edu

2008) percent reductions predicted. As these permafrost soils thaw, organic C is exposed to microbial degradation and released as CO₂ or methane, both greenhouse gases (Goulden and others 1998). Permafrost thaw may thus serve as a positive feedback to global climate change wherein warming causes soil thaw, releasing CO₂, which causes more warming (Schaefer and others 2011). In the first estimate based on field observations, effects of widespread permafrost thaw on raising atmospheric CO₂ levels by the end of this century may be equal to the current effect of deforestation (Schuur and others 2009).

High latitude ecosystems undergo numerous changes that affect their C balance when the permafrost underneath them begins to thaw. Generally, active layer (the amount of soil that thaws seasonally) depths deepen and soil temperatures rise, which can cause gross primary production and winter respiration to increase (Vogel and others 2009). In tundra, shrubs and mosses have been found to replace sedges as the dominant vegetation (Schuur and others 2007), while in peatlands, carpets of sphagnum moss have been found to form where thaw has caused bog collapse (Turetsky and others 2007). Although thaw can result in the mineralization of deep soil C (Goulden and others 1998; Dorrepaal and others 2009; Schuur and others 2009), which can be thousands of years old (Goulden and others 1998; Dutta and others 2006; Zimov and others 2006; Schuur and others 2009), warming associated with thaw can also increase net primary productivity (Natali and others, unpublished). Overall thaw-induced changes in ecosystems affect C inputs to the soil from plant litter and moss growth and C losses from the soils due to decomposition. Whether thaw causes permafrost-underlain ecosystems to become a net C source, releasing CO₂ to the atmosphere, or a net C sink, storing C in biomass and soils, ultimately depends on the balance between these inputs and outputs.

Scientists often use instantaneous CO₂ flux measurements of ecosystem respiration and gross primary production to determine whether permafrost ecosystems are a C source or sink. These flux measurements can be chamber-based (Goulden and others 1998; Wickland and others 2006) or from eddy covariance towers (Goulden and others 1998; Lund and others 2010). One chamber-based study demonstrated that tundra ecosystems increase their C sink capacity at the start of permafrost thaw but become C sources as thaw progresses (Vogel and others 2009). Direct measurements of C fluxes give estimates of an ecosystem's C balance (for example, net ecosystem production,

NEP) that can change annually (Goulden and others 1998) due to variable weather conditions. For robust estimates of ecosystem C balance using flux measurements, multi-year studies are needed. Furthermore, it can be difficult in cold systems to take the winter respiration measurements needed to calculate the annual net C balance using either chambers or eddy covariance (Lund and others 2010). Chamber-based and eddy covariance studies of permafrost systems often only measure winter respiration during a single month (Wickland and others 2006) or only measure growing season C fluxes (Turetsky and others 2007; Huemmrich and others 2010). Neglecting or under sampling winter respiration in high latitude ecosystems can lead to an incomplete understanding of C balance because wintertime respiration fluxes, though low, occur for a much longer duration than growing season respiration (Vogel and others 2009).

Alternatively, soil C accumulation rate measurements have been used to evaluate longer term ecosystem C balance. Several studies have investigated the response of C accumulation rates to recent climatic changes (Trumbore and Harden 1997; Turetsky and others 2007; O'Donnell and others 2011). Turetsky and others (2007) found collapsed bogs that had lost surface permafrost had increased organic matter accumulation rates and therefore increased surface C storage. Such measurements are advantageous in addition to direct C flux measurements because they integrate C balance over many years and thus give a decadal C balance (Trumbore and Harden 1997). But surface C accumulation rates do not account for deep soil decomposition and therefore do not measure NEP (Turetsky and others 2007). More C can be lost from deep soil than is accumulating in surface soil leading to a negative C balance but a positive C accumulation rate. However, decadal net C accumulation rates that include deep soil decomposition, and therefore estimate NEP, can be calculated when both recent and long-term C accumulation rates from a soil are known (Trumbore and Harden 1997). Decadal NEP more accurately measures net ecosystem C balance than surface C accumulation rates but cannot take into account recent changes to deep soil decomposition.

To predict future responses of soil organic carbon to climate change, we must know the quantity of soil C currently stored and its response to recent climatic changes (Schuur and others 2008; Trumbore and Czimczik 2008). To accomplish this, we chose to quantify surface and deep soil C stocks, inputs, and accumulation rates in a permafrost thaw gradient near Eight Mile Lake in Healy,

Alaska. Within this gradient, some areas have been undergoing thaw for at least two decades whereas others have only begun to thaw recently (Osterkamp and others 2009). We inventoried the amount of C stored in these soils to 1 m and compared how much relative diagenesis has already occurred in these soils based on their C:N and stable isotope depth profiles. We used radiocarbon dates and C inventories to model how permafrost thaw has affected soil C accumulation and compared decadal C accumulation rates to millennial C accumulation rates. We hypothesized that this permafrost-affected ecosystem's C balance calculated from accumulation models will show these soils have remained a C sink during the past five decades of climatic change. Finally, we compared decadal C balance calculated from C accumulation models to recent annual C balance calculated from flux measurements.

METHODS

Study Area

Our study area is a permafrost thaw gradient located near Eight Mile Lake (EML, 63° 52'42"N, 149° 15'12"W) in Healy, Alaska. The thaw gradient contains three sites named *minimal*, *moderate*, and *extensive* for the amount of vegetation change, active layer thickening, and thermokarst formation they have undergone due to different durations of permafrost thaw (Vogel and others 2009). At the extensive thaw site, permafrost thaw has been documented for the past two decades but likely began earlier (Osterkamp and others 2009). The vegetation is moist acidic tussock tundra underlain by soils that have permafrost within a meter of the surface (Gelisols). The soils consist of about 0.5 m of organic soil on top of mineral soil that is a mixture of loess deposits and glacial till (Vogel and others 2009). Permafrost temperatures in this region are around -1°C and therefore susceptible to thaw (Osterkamp and Romanovsky 1999). The permafrost thaw gradient has ongoing monitoring of soil temperature, permafrost thaw depth, water table depth, and CO_2 fluxes that have been measured regularly from May through September for the past 6 years (Schuur and others 2009; Vogel and others 2009).

Core Collection and Processing

We collected six soil cores each at extensive, moderate, and minimal thaw sites in May 2004. In areas without thermokarst, thawed soil was cut out in rectangular chunks using a bread knife. Chunk

dimensions were measured from the hole left in the ground. Inside thermokarsts, a Reeburgur soil corer with a 36.8 cm diameter was used to core thawed soil. Frozen soil was cored using a Tanaka drill with a 7.6 cm diameter hollow bit. The lengths cored ranged from 50 to 90 cm because we stopped coring when the corer hit small rocks within the loess, and the depth where rocks stopped the corer varied. Cores were wrapped in aluminum foil and kept frozen until lab processing.

In the lab, cores were weighed, thawed to be split into depth sections, and subsampled. Cores were split into the following depths: 0–5, 5–15, 15–25, 25–35, 35 cm to the end of the organic horizon, and 10 cm increments from the start of mineral soil until the end of the core. The organic/mineral horizon demarcation was determined visually and confirmed by %C analysis when the %C of the soil decreased to less than 20. Lengthwise slices of the core were refrozen for further analyses such as radiocarbon dating, and a slice was taken for moisture content and bulk %C, %N, $\delta^{13}\text{C}$, and $\delta^{15}\text{N}$ analyses. To determine moisture content, we weighed a subsample of soil before and after drying in a 60°C oven for 3 days (organic soils) or a 100°C oven for 24 h (mineral soils). Dried organic soil was ground on a Wiley Mill while dried mineral soil was ground with a mortar and pestle. Ground soils were run on a Costech Analytical ECS 4010 elemental analyzer coupled to a Finnigan Delta Plus XL stable isotope ratio mass spectrometer to obtain %C, %N, $\delta^{13}\text{C}$, and $\delta^{15}\text{N}$ values.

To determine bulk density, the dry mass of depth sections were divided by the field dimensions of rectangular chunks or corer dimensions then multiplied by section lengths. To determine C pools on a kg C m^{-2} basis, the bulk density was multiplied by the %C and divided by the height of each section. We calculated %C and %N in organic and mineral layers using bulk-density weighted averages of the depth sections and calculated $\delta^{13}\text{C}$ and $\delta^{15}\text{N}$ using weighted averages based on the amount C or N in a depth section. To calculate C pools to a constant depth of 1 m, we extrapolated mineral pools in cores that were less than 1 m long. We divided the sum of the C pools in the mineral horizon by the depth of the mineral measured and multiplied by the depth needed to obtain a 1 m core. We used an average of all 10 cm mineral layers in the core to extrapolate because pool sizes did not significantly change with depth in the mineral horizon. For comparisons of C pools, C:N ratios, and isotopic signatures among extensive, moderate, and minimal thaw sites, we performed ANOVAs with site and depth as main effects and a

site \times depth interaction in JMP 7 (SAS Institute, Cary, North Carolina).

Carbon accumulation rates

To calculate millennial and decadal soil C accumulation rates, we modeled cumulative C inventories versus age using data from deep and surface soils, respectively. We then used parameters from both the millennial and the decadal models to calculate decadal NEP. Radiocarbon values were used to age soil segments in each core. For ^{14}C analyses of decadal C accumulation rates, we used two cores from each site—cores 1 and 2 were from minimal thaw, cores three and four were from moderate thaw, and cores five and six were from extensive thaw. The cost of radiocarbon dating limited the number of replicates we could have. We sectioned cores into 1 cm segments from 0 to 5 cm and into 2 cm segments thereafter. From each section, we sorted out recognizable moss pieces. Holocellulose was extracted from a subset of the moss segments (five to six per core) using a modified Jayme–Wise method wherein the moss is extracted with toluene and ethanol then bleached with sodium hypochlorite (Gaudinski and others 2005). Moss was used to date surface soil segments because moss accretes vertically in situ unlike bulk organic matter, which has vascular inputs. We dated moss cellulose specifically because the atoms in cellulose do not undergo exchange with newer photosynthate once fixed. Because moss cellulose was used to date layers whereas the total C inventory included vascular plant detritus, this method assumes moss and vascular plant inputs decompose at the same rate (Trumbore and Harden 1997).

Four to five additional samples were chosen along the whole profiles of core two (minimal thaw) and core three (moderate thaw) to calculate millennial accumulation rates. For millennial rates, we plucked moss from 2 cm segments until we could no longer find enough recognizable moss (around 15–20 cm), then used 2 cm bulk samples for the rest of the organic layer, and 10 cm bulk samples for the mineral layer. We used bulk samples for millennial rates because the several-year difference between when vascular plant litter was fixed and when the litter entered the soil is inconsequential on millennial timescales. All moss cellulose and bulk soil samples were combusted inside pre-combusted, evacuated quartz tubes with cupric oxide (Vogel and others 1987; Dutta and others 2006). The resulting air mixture was purified into CO_2 using liquid N_2 on a vacuum line before reducing the CO_2 into graphite by Fe reduction in He (Vogel and others 1987).

Graphite samples were sent to the UC Irvine W. M. Keck Carbon Cycle Accelerator Mass Spectrometry Laboratory for $\Delta^{14}\text{C}$ analysis.

Modern (post 1950) $\Delta^{14}\text{C}$ values were referenced against the atmospheric radiocarbon record from Hua and Barbetti (2004) to obtain calendar ages for the moss cellulose samples and subsequently each soil segment. Pre-1950 ages of moss cellulose and bulk samples were obtained using the InCal09 calibration dataset in Calib 6.0 (Stuiver and Reimer 2010). We added 3 years to modern segment ages to correct for time it takes newly fixed C in live green moss to become brown moss detritus (Osterkamp and others 2009). For moss and bulk samples, we assigned the age to the midpoint of each segment.

To calculate C accumulation rates, we fitted the ^{14}C -age model described in Trumbore and Harden (1997). This model assumes a net change in C storage (dC/dt) is a balance between annual C inputs (I) and decomposition (kC):

$$\frac{dC}{dt} = I - kC \quad (1)$$

When solved, this equation becomes:

$$C_t = C_0 * e^{-kt} + \frac{I}{k} * (1 - e^{-kt}) \quad (2)$$

where C_0 is the initial C pool (g C m^{-2}), C_t is the inventory of C in a given core as of year t (g C m^{-2} ; the year sampled (2004) minus the calendar age), I is the annual C inputs ($\text{g C m}^{-2} \text{ y}^{-1}$), and k is the first-order decomposition rate constant (y^{-1}). The model was fitted to plots of cumulative C inventory (C_t) versus time for each core using the nls function in R (R Core Development Team 2011) to obtain estimates for I and k , which were used to calculate turnover time and accumulation rates.

The millennial C accumulation curves crossed the origin, so the initial C pool was zero and the $C_0 * e^{-kt}$ term in equation (2) dropped out. However, the decadal C accumulation curves did not cross the origin and needed a negative C_0 for the model to converge. Although correct mathematically, conceptually this result was nonsensical because a negative initial C pool is not possible. To fit the decadal data, the model needed to be shifted to the right on the x -axis, so we dropped the $C_0 * e^{-kt}$ term and added an x intercept, t_i , to the model:

$$C_t = \frac{I}{k} * (1 - e^{-k(t-t_i)}) \quad (3)$$

This modified equation gave the same parameter estimates as equation (2) without needing a negative initial C pool. The parameter t_i can be

interpreted as the number of years before sampling (2004) that measurable C accumulation stopped. For cores 1, 2, 5, and 6, the oldest data points were dropped from the decadal analyses because they prevented model convergence. These data points (from 5–7 or 7–9 cm segments) were likely sampled too coarsely at depth increments that included the increasing slope of the bomb peak. In these segments, a small amount of modern $\Delta^{14}\text{C}$ could dominate the $\Delta^{14}\text{C}$ signature leading to erroneously young estimated ages.

Estimates of decadal NEP were calculated by subtracting decomposition of deep soil from decadal C accumulation rates (Trumbore and others 1999):

$$\text{NEP} = I_{\text{decadal}} - k_{\text{decadal}} * C_{\text{shallow}} - k_{\text{millennial}} * C_{\text{deep}} \quad (4)$$

where I_{decadal} and k_{decadal} are the C input rate and decomposition constant, respectively, from the decadal C accumulation model, C_{shallow} is the C pool in the surface soil, $k_{\text{millennial}}$ is the decomposition constant from the millennial C accumulation model, and C_{deep} is the C pool in the deep soil. For equation (4) and decadal C accumulation rate calculations, C_{shallow} is the amount of C from the soil surface to the end of the depths used to fit parameters in equation (2), which varies by core (4 cm in core 1; 5 cm in cores 2, 5, and 6; and 7 cm in cores 3 and 4). For equation (4) and millennial C accumulation rate calculations, C_{deep} is the amount of C from the end of the modeled shallow depths until the start of permafrost because we assumed minimal microbial activity within frozen soil. To calculate NEP for cores 1, 4, 5, and 6, an average of the millennial decomposition constants was used.

RESULTS

C Inventories

Carbon pools at all sites were large, exceeding 50 kg C m⁻² in the first meter. Carbon pools in

both the top 1 m and the active layer of soils were greatest in moderate thaw but the effect was only marginally significant for the top meter (Table 1, $P = 0.062$ and $P = 0.011$, respectively). Minimal thaw had the least amount of C stored in the organic soil horizons, but again the effect was only marginally significant (Table 1, $P = 0.059$), and minimal thaw had a shallower organic horizon than extensive thaw (Table 1, $P = 0.016$). Active layer depths ranged from 62 cm in minimal thaw to 73 cm in extensive thaw (Table 1).

Soil Profiles

All cores showed a significant increase in bulk density with depth, but bulk density did not differ among sites (Table 2, two-way ANOVA, depth effect, $P < 0.0001$, site effect $P = 0.69$). Similarly, %C decreased significantly with depth but did not differ among sites (Table 2, two-way ANOVA, depth effect $P < 0.0001$, site effect, $P = 0.53$). Carbon percentages increased in most cores within the mineral soil, sometimes above 20%, the threshold for classification as an organic soil, indicating buried organic layers (Figure 1). At all sites, %N was greatest in the bottom of the organic layer and least in the mineral layer (Table 2, two-way ANOVA, depth effect $P < 0.0001$, site effect, $P = 0.94$). Site by depth interactions were not significant.

For C:N ratios, there were no differences among sites (Figure 2, two-way ANOVA, site effect, $P = 0.48$) but there were significant differences among depths (depth effect, $P < 0.0001$). Within organic layers, C:N ratios were highest in the 0–5 cm and 5–15 cm layers, lowest in the 25–35 cm and 35+ cm layers, and constant within mineral layers. Unlike other parameters, there was a significant site effect for $\delta^{13}\text{C}$ with minimal thaw being more enriched than extensive thaw (Figure 2, two-way ANOVA, site effect, $P = 0.0014$). Also, at all sites $\delta^{13}\text{C}$ was most enriched in the bottom organic layers and most depleted at the top of the organic and in the

Table 1. Mean (Standard Error) Organic Soil Depth, Active Layer Depth, and C Inventory

Site	Org depth (cm)	Active layer ¹ (cm)	C pool to 1 m (kg C m ⁻²)	Org C pool (kg C m ⁻²)	Active Layer C pool (kg C m ⁻²)
Minimal	37 (3.1) ^a	62.2 (1)	55.7 (4.1) ^a	18.6 (2.3) ^a	35.0 (1.5) ^a
Moderate	49 (5.9) ^{ab}	65.8 (1)	68.5 (5.3) ^a	33.0 (5.8) ^a	45.8 (2.5) ^b
Extensive	54 (4.8) ^b	72.6 (0.8)	54.6 (3.0) ^a	28.4 (4.4) ^a	40.1 (2.1) ^{ab}

¹2009 Data from Trucco (unpublished). ($n = 6$). Letters not shared among sites indicate significant differences (one-way ANOVA, $\alpha < 0.05$).

Table 2. Mean (Standard Error) Bulk Density, %C, and %N for Organic and Mineral Soil

Site	Depth	Bulk density (g cm^{-3})	Carbon (%)	Nitrogen (%)
Minimal	0–15 cm org	0.070 (0.007) ^a	42.2 (0.69) ^a	0.93 (0.04) ^a
	15–35+ cm org	0.17 (0.02) ^b	37.4 (0.60) ^b	1.59 (0.06) ^b
	Mineral	0.53 (0.07) ^c	12.6 (2.7) ^c	0.49 (0.1) ^c
Moderate	0–15 cm org	0.071 (0.005) ^a	42.1 (0.30) ^a	0.80 (0.07) ^a
	15–35+ cm org	0.22 (0.02) ^b	37.6 (1.2) ^b	1.68 (0.06) ^b
	Mineral	0.46 (0.05) ^c	13.6 (2.4) ^c	0.52 (0.09) ^c
Extensive	0–15 cm org	0.056 (0.006) ^a	41.6 (0.26) ^a	0.88 (0.08) ^a
	15–35+ cm org	0.18 (0.02) ^b	35.2 (1.4) ^b	1.49 (0.04) ^b
	Mineral	0.46 (0.05) ^c	12.4 (2.2) ^c	0.57 (0.1) ^c

The deeper organic layer was labeled 35+ because the depth of the organic horizon varied by core. Letters not shared among depths indicate significant differences (two-way ANOVA, $\alpha < 0.05$). There were no significant differences among sites ($n = 6$).

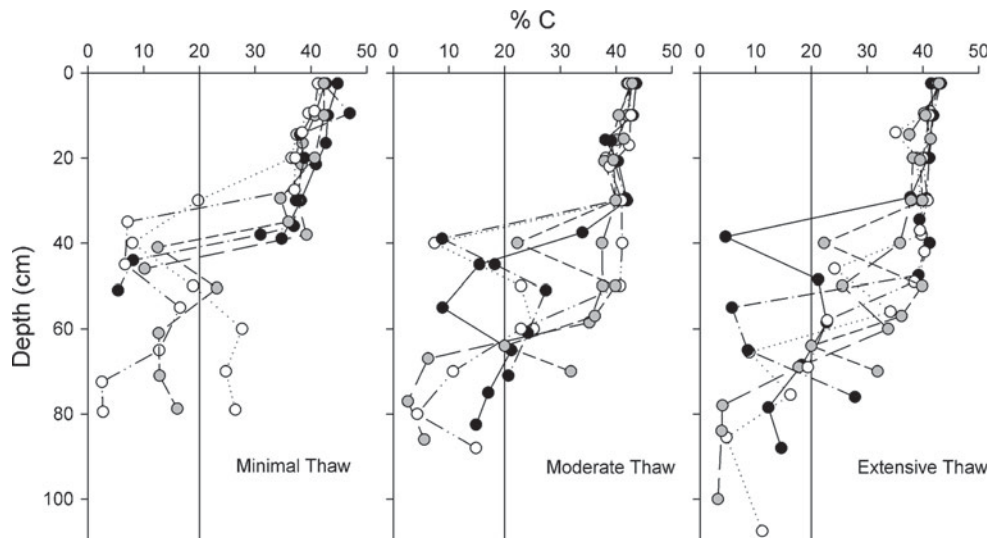


Figure 1. Depth profiles for each core taken at minimal, moderate, and extensive permafrost thaw sites. The depth is the middle of the layer in which %C was measured. Note the high %C at depth, which often exceeds 20% (black vertical lines, the threshold used to categorize organic from mineral soil) and indicates cryoturbation of organic soil into mineral horizons. Not all profiles are the same length because of variance in the depth where small rocks inhibited further coring.

mineral layers (Figure 2, two-way ANOVA, depth effect, $P < 0.0001$). $\delta^{15}\text{N}$ did not differ among sites (Figure 2, two-way ANOVA, site effect, $P = 0.77$) but did differ with depth (depth effect, $P < 0.0001$) becoming more enriched from the 0–5 cm to 15–25 cm organic layer, after which it remained constant through the mineral layers.

C Accumulation Rates

Profiles of $\Delta^{14}\text{C}$ in surface and deep soils were used to date soil core segments for decadal and millennial C accumulation models, respectively

(Figure 3). Radiocarbon values peak within the first 5 cm of each core, which generally corresponds to the bomb peak of 1963—the year of increased atmospheric nuclear weapons testing before the test ban went into effect (Levin and Hesshaimer 2000). The location of the $\Delta^{14}\text{C}$ peak in each surface profile is similar between cores sampled from the same site but differ across sites: minimal thaw cores have $\Delta^{14}\text{C}$ peaks closest to the surface, extensive thaw cores have $\Delta^{14}\text{C}$ peaks farthest from the surface at 5 cm, and the $\Delta^{14}\text{C}$ peaks of moderate thaw cores fall in between (Figure 3A). The deep soil $\Delta^{14}\text{C}$ profiles

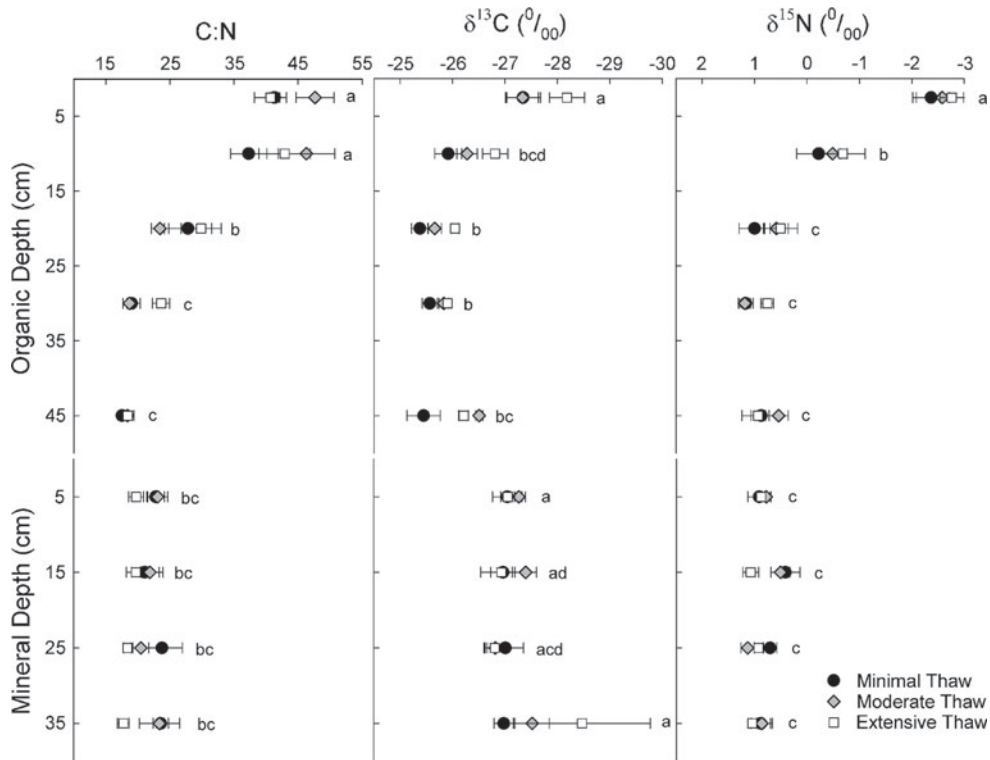


Figure 2. Mean C:N, $\delta^{13}\text{C}$, and $\delta^{15}\text{N}$ of organic (*top*) and mineral (*bottom*) soil layers at the minimal, moderate, and extensive thaw sites. The depths start over again for the mineral layer because the organic layer does not have a uniform thickness. Error bars represent the standard error. $n = 6$ in organic layers but varies from two to six in mineral layers due to varying core lengths. Depths that do not share a letter are significantly different (two-way ANOVA, $\alpha = 0.05$). The only significant difference among sites was that minimal thaw was more ^{13}C enriched than extensive thaw.

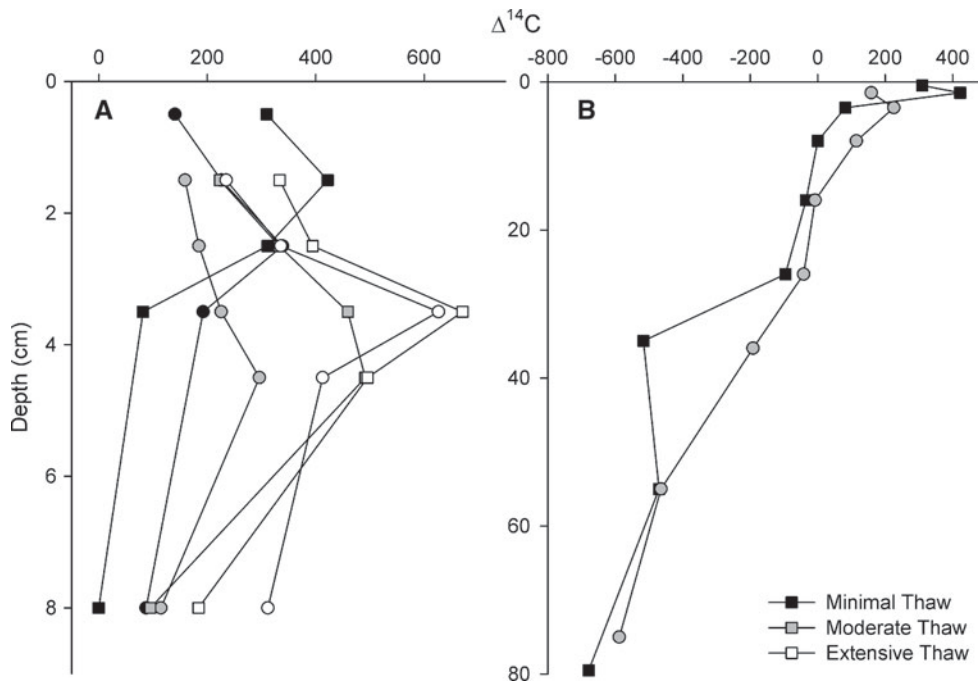


Figure 3. Depth profiles of radiocarbon values used to calculate ages for decadal (**A**) and millennial (**B**) C accumulation models. The increase in $\Delta^{14}\text{C}$ found in the surface profiles show where radiocarbon from the nuclear weapons testing bomb peak (circa 1963) was fixed. Negative radiocarbon values found in deep profiles indicate the radiocarbon has undergone radioactive decay since it was fixed. The $\Delta^{14}\text{C}$ at the bottom of the cores (**B**) correspond to calendar ages of 8,000–10,000 years ago.

(Figure 3B) from cores 2 and 3 are similar to one another. The $\Delta^{14}\text{C}$ values at the bottom of the core correspond to calendar ages of 8,000–10,000 years ago. Core 2 has a deviation in $\Delta^{14}\text{C}$ that is likely due to cryoturbation.

Modeled decadal C accumulation rates for EML soils ranged from 6.84 to 41.6 $\text{g C m}^{-2} \text{y}^{-1}$

(Table 3; Figure 4). Carbon inputs ranged from 42.3 to 140 $\text{g C m}^{-2} \text{y}^{-1}$. The decomposition rate constant (k) ranged from 0.031 to 0.064, excluding core 2. Turnover times were decadal ranging from 16 to 32 years, excluding core 2. The x intercept, t_i , ranged from 7.5 to 18 years before sampling. The average decadal C accumulation rate, C inputs, and

Table 3. Inputs (I), Decomposition Constants (k), and Accumulation Rates from Decadal and Millennial Models

Core	I ($\text{g C m}^{-2} \text{y}^{-1}$)	SE		k (y^{-1})	SE		t_i (year)	TT (year)	C acc ($\text{g C m}^{-2} \text{y}^{-1}$)
		Upper	Lower		Upper	Lower			
Decadal									
1	83.0	110	63	0.050	0.07	0.03	7.48 (1.7)	19.9	6.84
2	42.3	140	13	0.0015	1	0.00	17.0 (7.3)	669	39.9
3	140	150	130	0.064	0.07	0.05	8.40 (0.55)	15.7	14.3
4	109	150	80	0.032	0.06	0.02	12.3 (2.6)	31.5	41.6
5	43.1	56	33	0.031	0.06	0.02	10.2 (1.5)	32.2	14.3
6	105	512	21	0.041	0.65	0.001	18.0 (9.0)	24.5	37.9
Millennial									
2	13	16	11	0.00032	0.00041	0.00025		3090	2.19
3	12	19	8.0	0.00030	0.00057	0.00016		3330	2.39

TT = Turnover times and C acc = C accumulation rates were calculated from the fitted parameters. I and k have upper and lower standard errors that are not symmetrical around the estimate because they were fitted as natural logs to avoid placing non-zero bounds on the parameters. t_i is the x intercept from the decadal models. Cores 1 and 2 are from minimal thaw, cores 3 and 4 are from moderate thaw, and cores 5 and 6 are from extensive thaw. Decadal C accumulation rates are calculated from 0 to end of the modeled depth (4 cm in core 1; 5 cm in cores 2, 5, and 6; and 7 cm in cores 3 and 4). Millennial rates are calculated from the end of depths modeled for decadal accumulation to the bottom of the active layer (Table 1).

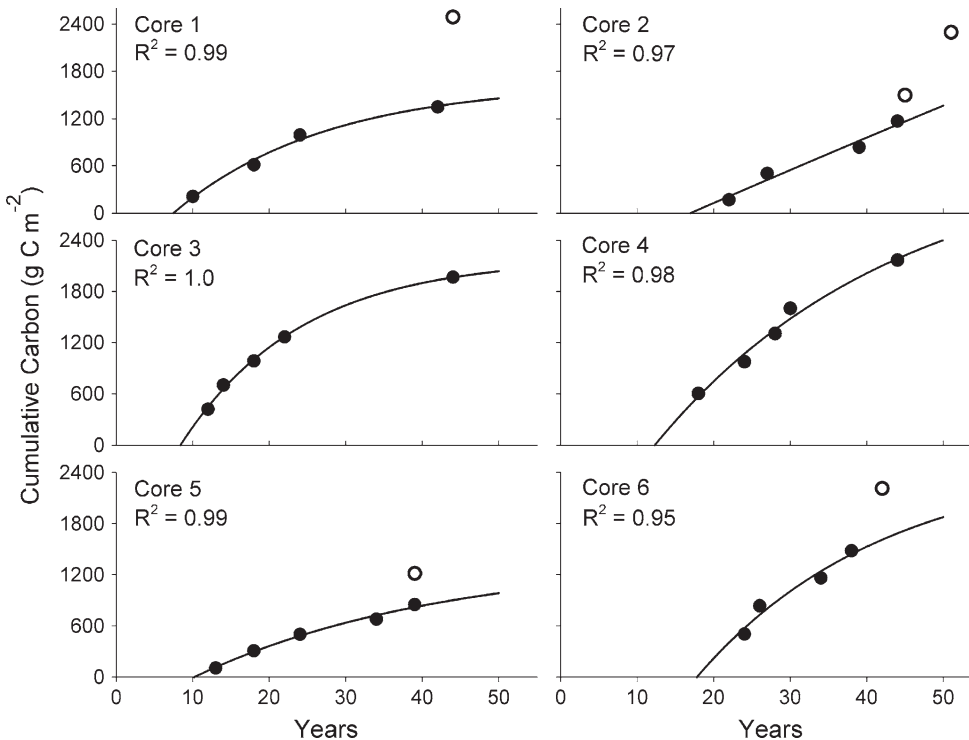


Figure 4. Cumulative C inventories versus the age of C in that soil layer. All points were used to fit the accumulation model (equation 2) except for the oldest point(s) (open circles) in cores 1, 2, 5, and 6, which were excluded from the analyses (see text). Curves are the predicted values calculated from estimated I , k , and t_i values (Table 3). Cores 1 and 2 are from minimal thaw, cores 3 and 4 are from moderate thaw, and cores 5 and 6 are from extensive thaw.

turnover times for EML soils were $25.8 \text{ g C m}^{-2} \text{y}^{-1}$, $87 \text{ g C m}^{-2} \text{y}^{-1}$, and 25 years (excluding core 2), respectively.

Millennial scale C accumulation rates were an order of magnitude less than decadal rates, ranging from 2.2 to $2.4 \text{ g C m}^{-2} \text{y}^{-1}$ (Table 3; Figure 5). Carbon input rates were similar in both cores ($12\text{--}13 \text{ g C m}^{-2} \text{y}^{-1}$), less than, but within the same

order of magnitude as, decadal C input rates. The decomposition constants for these millennial accumulation rates were two orders of magnitude less than decadal accumulation rates leading to turnover times on the order of three thousand years (Table 3). Decadal NEP at EML averaged $14.4 \text{ g C m}^{-2} \text{y}^{-1}$ but ranged over an order of magnitude (Table 4; Figure 6).

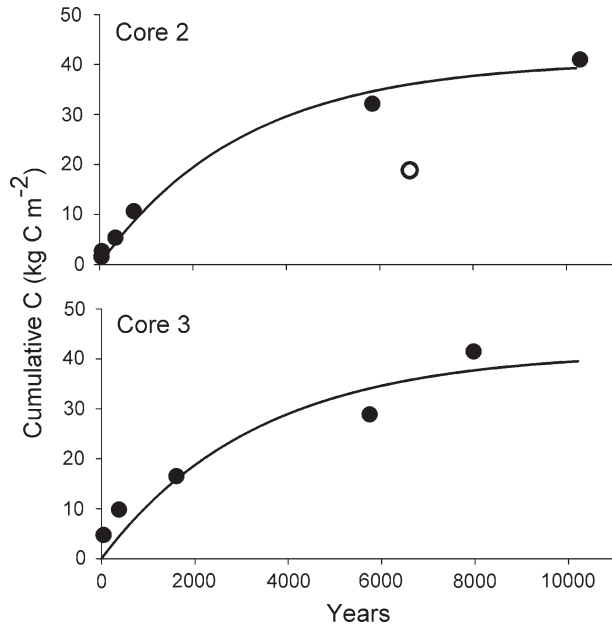


Figure 5. Cumulative C inventories versus the age of C in that soil layer. All points were used to fit the accumulation model (equation 2) except for one point from core 2 (as indicated by the *open circle*) which was excluded from the analysis as an outlier due to cryoturbation. Curves are the predicted values calculated from estimated I and k values (Table 3).

DISCUSSION

C Inventories and Depth Profiles

Carbon inventories in the top meter at EML ranged from 55 to 69 kg C m^{-2} , within the upper half of the 16–94 kg C m^{-2} range reported for similar tundra soils across Alaska (Michaelson and others 1996). Active layer carbon pools and the percentage of the 1 m C inventory exposed by the active layer (63–71%) were also within ranges for Alaskan and Canadian arctic soils (Michaelson and others 1996; Hugelius and others 2010). The permafrost at EML held a lot of C due to high C concentrations (20–30%) within the “mineral” horizon. High %C in mineral horizons is common among permafrost-affected soils because organic material is mixed into deeper horizons by cryoturbation where it becomes protected from further decomposition (Ping and others 2010). The active layer C pool was larger in moderate thaw than in minimal thaw, but did not increase further in extensive thaw because extensive thaw had a lower C density (C per gram of soil). Despite extensive thaw’s lower C density, the percentage of the 1 m C pool contained in the active layer at EML increased from 63 in minimal thaw to 71 in extensive thaw due to extensive thaw’s thicker active layer.

Table 4. Decadal NEP and the Soil C Pools Used to Calculate NEP

Core	C_{shallow} (kg m^{-2})	C_{deep} (kg m^{-2})	NEP ($\text{g C m}^{-2} \text{ yr}^{-1}$)
1	1.52	28.0	−1.98
2	1.66	34.0	28.9
3	1.97	33.4	4.08
4	2.13	41.9	28.4
5	0.93	38.6	2.12
6	1.64	40.9	25.0

The shallow and deep C inventories for each core were also used to solve for each core’s decadal and millennial C accumulation rates, respectively.

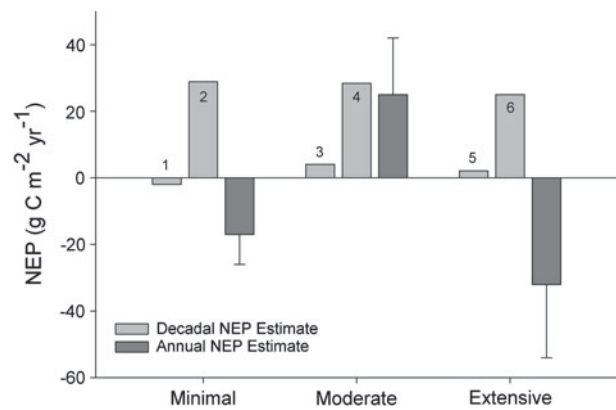


Figure 6. Decadal Net Ecosystem Production (NEP) for two cores at each site in the thaw gradient and annual NEP calculated from recent flux measurements at the thaw gradient averaged over 3 years (Vogel and others 2009). Positive NEP indicates the ecosystem is a C sink whereas negative NEP indicates the ecosystem is a C source.

Assuming extensive thaw once had an active layer that was a similar depth to minimal thaw, an additional 6.4 kg C m^{-2} has been made available to above-freezing decomposition due to permafrost thaw.

Within the organic layer at all sites, C:N decreased and $\delta^{13}\text{C}$ and $\delta^{15}\text{N}$ became more enriched with depth, indicating increasing degrees of decomposition (Figure 2; Kuhry and Vitt 1996; Bostrom and others 2007; Hobbie and Ouimette 2009). Carbon to nitrogen ratios decrease over the decomposition process because C is lost from the soil as it is mineralized, whereas N, though it may change form, generally stays within the soil (Malmer and Holm 1984; Sterner and Elser 2002). Loss pathways of C and N from soil typically favor lighter isotopes, so more heavy isotopes relative to

light isotopes remain over time as organic matter is decomposed (Bostrom and others 2007; Hobbie and Ouimette 2009). In the organic horizon, minimal thaw was more ^{13}C -enriched than extensive thaw indicating they have different soil organic matter sources, not that decomposition is greater at minimal thaw, because C:N and $\delta^{15}\text{N}$ did not differ. Minimal thaw is dominated by graminoids with a $\delta^{13}\text{C}$ of -25‰ , whereas extensive thaw is dominated by shrubs and mosses with a $\delta^{13}\text{C}$ around -29‰ (Schuur and others 2007, unpublished data). Within the mineral layer C:N, $\delta^{13}\text{C}$, and $\delta^{15}\text{N}$ remained constant, indicating little additional decomposition was occurring in this cryo-protected layer—all but the top of which is within permafrost. This lack of decomposition in the permafrost leads to the buildup of deep soil C that is 8,000–10,000 years old.

C Accumulation Rates

Eight Mile Lake tundra soils have substantial decadal and millennial rates of C accumulation indicating they have been active C sinks from the early Holocene through the most of the past 50 years (Table 3). Considering the six cores across the gradient together, EML soils had decadal C inputs within ranges reported for nutrient poor bogs and black spruce forests (Trumbore and Harden 1997; O'Donnell and others 2011). Decadal decomposition rate constants (k) were generally within previously reported values for boreal forest sites with moss cover, which range from 0.0001 to 0.045 y^{-1} (Trumbore and Harden 1997; O'Donnell and others 2011). Carbon accumulation rates in EML soils also fell within values for boreal forests and wetlands, which range from 3 to 260 $\text{g C m}^{-2} \text{y}^{-1}$ (Trumbore and Harden 1997; O'Donnell and others 2011). The similarities among C input rates, decomposition constants, and C accumulation rates across these subarctic ecosystems likely result from their similar poorly drained surface soils dominated by recalcitrant mosses and underlain by shallow permafrost.

Millennial C accumulation rates in EML tundra soils were similar to deep soil C accumulation rates in boreal wetland and forest soils, but deep soil C inputs and decomposition constants differed (Trumbore and Harden 1997; O'Donnell and others 2010). EML had lower C inputs to deep soils than Canadian boreal forests and wetlands (Trumbore and Harden 1997). Lower C inputs to deep soils may be due to the shallower active layer at EML than in boreal forests and wetlands, which causes cryoturbation, not root growth, to be the

main mechanism transporting C from the surface to deep soil. The shallower active layer also explains the lower deep soil decomposition constants at EML, because more deep soil is cryoprotected. In contrast, EML had deep soil C inputs an order of magnitude higher than mineral and permafrost soils of an Alaskan black spruce forest but had similar deep soil decomposition constants (O'Donnell and others 2010). EML soils had a larger deep C pool than this Alaskan black spruce forest (about 34 kg C vs. 6–10 kg C) and therefore more deep soil decomposition overall, which is how EML could have similar millennial C accumulation rates (about 2 $\text{g C m}^{-2} \text{y}^{-1}$) despite having much greater C inputs.

Carbon input and decomposition rates are related wherein greater C inputs coincide with larger decomposition losses at individual sampling points across this landscape (Figure 7). Carbon inputs in this model are analogous to net primary production (NPP) of the tundra ecosystem. Environmental conditions that favor greater plant growth such as warm soil and air temperatures, moderate soil moisture, and high soil nutrient availability also favor greater microbial activity and therefore faster soil decomposition (Shaver and others 1992; Chapin and others 2002; Raich and others 2006). Conversely, low temperatures, dry or excessively wet soils, and low nutrient availability cause both decreased plant growth and microbial activity. This positive relationship appears to constrain variation in C accumulation rates across the landscape because high inputs are likely to be balanced by faster decomposition rates.

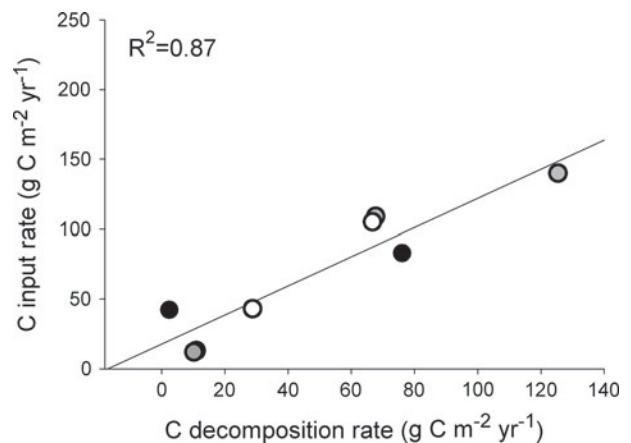


Figure 7. The relationship between C input (I , Table 3) and decomposition rates (kC , Tables 3, 4) for the six surface soils (decadal rates) and the two deep soils (millennial rates, bottommost points).

Net Ecosystem Production

Decadal NEP estimates calculated with parameters from decadal and millennial C accumulation models (equation 4) can be compared to annual NEP estimates calculated from ecosystem gas exchange measurements as a way to independently evaluate our model estimates. Decadal NEP calculated with this dataset averaged $14.4 \text{ g C m}^{-2} \text{ y}^{-1}$ (Table 4). These fluxes were within the range of decadal NEP at boreal forest sites, though much less than the maximum rate of $180 \text{ g C m}^{-2} \text{ y}^{-1}$ calculated for fen sites (Trumbore 1997; Trumbore and others 1999). Decadal estimates of NEP were similar to current annual estimates of NEP made with gas exchange measurements at EML, which ranged from -58 to $57 \text{ g C m}^{-2} \text{ y}^{-1}$ from 2004 to 2006 (Vogel and others 2009). Furthermore, estimates of the percentage of heterotrophic respiration coming from deep soil derived from the decadal NEP equation (10–30%) match previous estimates (7–23%) derived from partitioning respiration using radiocarbon measurements of ecosystem gas exchange (Schuur and others 2009).

Although the mean of decadal NEP estimates was positive indicating over the past five decades these soils were a C sink, it appears that surface C accumulation stopped 8–18 years ago. This estimate of 8–18 years is from the t_i parameter needed to fit the decadal C accumulation data. This deviation from conditions of steady accumulation may be interpreted as either a halting of recent soil C accumulation within surface soils (inputs balanced by outputs) or a shift of C inputs from vertical accumulation at the soil surface to deeper in the soil. The latter explanation would be consistent with surface moss growth being replaced by belowground vascular plant growth. In fact, a shift to more belowground NPP could also explain the outlier points in our decadal C accumulation data. The outlier layers were either younger than expected or had more C than expected by the average accumulation rate over the entire profile. Root biomass peaks within the 5–15 cm depth from which these outlier segments came (unpublished data). However, outliers were found in only four of the six cores, although surface accumulation stopped in all cores. The former explanation is supported by observed negative flux-derived annual NEP at all EML sites in 2005 and at extensive and minimal thaw in 2004 (Vogel and others 2009). If there were enough negative NEP years to counteract positive NEP years over the past two decades, then C inputs would roughly balance C outputs and C accumulation would be negligible. The estimate that vertical C accumulation halted

within the past two decades coincides with an era of permafrost warming at EML (Osterkamp and others 2009).

Overall, the deviation from steady vertical C accumulation after millenia indicates the C cycle in this tundra ecosystem is undergoing major change in response to permafrost warming and thaw. Tundra soils that were once a significant C sink are likely becoming a C source. Soils from minimal, moderate, and extensive thaw had positive decadal and millennial C accumulation rates demonstrating they have been accumulating C since the start of the Holocene (Figure 5). However, according to annual flux-derived estimates of NEP, all sites have been observed to be C sources during at least 1 year in the past decade, and based on a 3-year average, extensive and minimal thaw are C sources (Figure 6; Vogel and others 2009). Even one of our decadal NEP estimates (core 1) was negative indicating that decomposition in the deep soil has been outpacing C inputs from the surface soil. Furthermore, our decadal accumulation models indicate vertical soil C accumulation halted within the past 18 years. Thus, this shift in the C balance of these tundra soils is leading to increased atmospheric CO_2 concentrations through the microbial release of soil C to the atmosphere (Schuur and others 2009) and through the loss of C uptake these soils used to provide.

REFERENCES

- Bostrom B, Comstedt D, Ekblad A. 2007. Isotope fractionation and C-13 enrichment in soil profiles during the decomposition of soil organic matter. *Oecologia* 153:89–98.
- Chapin FS, Matson PA, Mooney HA. 2002. Principles of ecosystem ecology. New York: Springer.
- Dorrepal E, Toet S, van Logtestijn RSP, Swart E, van de Weg MJ, Callaghan TV, Aerts R. 2009. Carbon respiration from subsurface peat accelerated by climate warming in the subarctic. *Nature* 460:616–79.
- Dutta K, Schuur EAG, Neff JC, Zimov SA. 2006. Potential carbon release from permafrost soils of Northeastern Siberia. *Glob Change Biol* 12:2336–51.
- Gaudinski JB, Dawson TE, Quideau S, Schuur EAG, Roden JS, Trumbore SE, Sandquist DR, Oh SW, Wasylishen RE. 2005. Comparative analysis of cellulose preparation techniques for use with C-13, C-14, and O-18 isotopic measurements. *Anal Chem* 77:7212–24.
- Goulden ML, Wofsy SC, Harden JW, Trumbore SE, Crill PM, Gower ST, Fries T, Daube BC, Fan SM, Sutton DJ, Bazzaz A, Munger JW. 1998. Sensitivity of boreal forest carbon balance to soil thaw. *Science* 279:214–17.
- Hobbie EA, Ouimette AP. 2009. Controls of nitrogen isotope patterns in soil profiles. *Biogeochemistry* 95:355–71.
- Hua Q, Barbetti M. 2004. Review of tropospheric bomb C-14 data for carbon cycle modeling and age calibration purposes. *Radiocarbon* 46:1273–98.

- Huemmrich KF, Kinoshita G, Gamon JA, Houston S, Kwon H, Oechel WC. 2010. Tundra carbon balance under varying temperature and moisture regimes. *J Geophys Res Biogeosci* 115.
- Hugelius G, Kuhry P, Tarnocai C, Virtanen T. 2010. Soil organic carbon pools in a periglacial landscape: a case study from the Central Canadian Arctic. *Permafrost Periglac Process* 21:16–29.
- IPCC (Intergovernmental Panel on Climate Change). 2007. Climate Change 2007: the physical science basis. In: Solomon S, Qin D, Manning M, Chen Z, Marquis M, Avery KB, Tignor M, Miller HL, Eds. Contribution of Working Group I to the fourth assessment report of the IPCC. New York: Cambridge University Press.
- Kuhry P, Vitt DH. 1996. Fossil carbon/nitrogen ratios as a measure of peat decomposition. *Ecology* 77:271–5.
- Lawrence DM, Slater AG, Romanovsky VE, Nicolsky DJ. 2008. Sensitivity of a model projection of near-surface permafrost degradation to soil column depth and representation of soil organic matter. *J Geophys Res Earth Surf* 113:14.
- Levin I, Hesshaimer V. 2000. Radiocarbon—a unique tracer of global carbon cycle dynamics. *Radiocarbon* 42:69–80.
- Lund M, Lafleur PM, Roulet NT, Lindroth A, Christensen TR, Aurela M, Chojnicki BH, Flanagan LB, Humphreys ER, Laurila T, Oechel WC, Olejnik J, Rinne J, Schubert P, Nilsson MB. 2010. Variability in exchange of CO₂ across 12 northern peatland and tundra sites. *Glob Change Biol* 16:2436–48.
- Malmer N, Holm E. 1984. Variation in the C/N-Quotient of peat in relation to decomposition rate and age-determination with PB-210. *Oikos* 43:171–82.
- Michaelson GJ, Ping CL, Kimble JM. 1996. Carbon storage and distribution in tundra soils of Arctic Alaska, USA. *Arctic Alpine Res* 28:414–24.
- O'Donnell JA, Harden JW, McGuire AD, Kanevskiy MZ, Jorgenson MT, Xu XM. 2011. The effect of fire and permafrost interactions on soil carbon accumulation in an upland black spruce ecosystem of interior Alaska: implications for post-thaw carbon loss. *Glob Change Biol* 17:1461–74.
- Osterkamp TE, Jorgenson MT, Schuur EAG, Shur YL, Kanevskiy MZ, Vogel JG, Tumskey VE. 2009. Physical and ecological changes associated with warming permafrost and thermokarst in interior Alaska. *Permafrost Periglac Process* 20:235–56.
- Osterkamp TE, Romanovsky VE. 1999. Evidence for warming and thawing of discontinuous permafrost in Alaska. *Permafrost Periglac Process* 10:17–37.
- Ping CL, Michaelson GJ, Kane ES, Packee EC, Stiles CA, Swanson DK, Zaman ND. 2010. Carbon stores and biogeochemical properties of soils under black spruce forest, Alaska. *Soil Sci Soc Am J* 74:969–78.
- R Development Core Team. 2011. R: a language and environment for statistical computing. R Foundation for Statistical Computing, Vienna, Austria. ISBN 3-900051-07-0. <http://www.R-project.org>.
- Raich JW, Russell AE, Kitayama K, Parton WJ, Vitousek PM. 2006. Temperature influences carbon accumulation in moist tropical forests. *Ecology* 87:76–87.
- Schaefer K, Zhang T, Bruhwiler L, Barrett AP. 2011. Amount and timing of permafrost carbon release in response to climate warming. *Tellus B* 63:165–80.
- Schuur EAG, Bockheim J, Canadell JG, Euskirchen E, Field CB, Goryachkin SV, Hagemann S, Kuhry P, Lafleur PM, Lee H, Mazhitova G, Nelson FE, Rinke A, Romanovsky VE, Shiklomanov N, Tarnocai C, Venevsky S, Vogel JG, Zimov SA. 2008. Vulnerability of permafrost carbon to climate change: implications for the global carbon cycle. *Bioscience* 58:701–14.
- Schuur EAG, Crummer KG, Vogel JG, Mack MC. 2007. Plant species composition and productivity following permafrost thaw and thermokarst in Alaskan tundra. *Ecosystems* 10:280–92.
- Schuur EAG, Vogel JG, Crummer KG, Lee H, Sickman JO, Osterkamp TE. 2009. The effect of permafrost thaw on old carbon release and net carbon exchange from tundra. *Nature* 459:556–9.
- Shaver GR, Billings WD, Chapin FS, Giblin AE, Nadelhoffer KJ, Oechel WC, Rastetter EB. 1992. Global change and the carbon balance of arctic ecosystems. *Bioscience* 42:433–41.
- Sterner RW, Elser JJ. 2002. Ecological stoichiometry. Princeton (NJ): Princeton University Press.
- Stuiver M, Reimer P. 2010. Calib 14C Calibration Program. <http://calib.qub.ac.uk/calib>.
- Tarnocai C, Canadell JG, Schuur EAG, Kuhry P, Mazhitova G, Zimov S. 2009. Soil organic carbon pools in the northern circumpolar permafrost region. *Global Biogeochem Cycles* 23:11.
- Trumbore SE. 1997. Potential responses of soil organic carbon to global environmental change. *Proc Natl Acad Sci USA* 94:8284–91.
- Trumbore SE, Bubier JL, Harden JW, Crill PM. 1999. Carbon cycling in boreal wetlands: A comparison of three approaches. *J Geophys Res Atmos* 104:27673–82.
- Trumbore SE, Czimczik CI. 2008. Geology—an uncertain future for soil carbon. *Science* 321:1455–6.
- Trumbore SE, Harden JW. 1997. Accumulation and turnover of carbon in organic and mineral soils of the BOREAS northern study area. *J Geophys Res Atmos* 102:28817–30.
- Turetsky MR, Wieder RK, Vitt DH, Evans RJ, Scott KD. 2007. The disappearance of relict permafrost in boreal north America: effects on peatland carbon storage and fluxes. *Glob Change Biol* 13:1922–34.
- Vogel J, Schuur EAG, Trucco C, Lee H. 2009. Response of CO₂ exchange in a tussock tundra ecosystem to permafrost thaw and thermokarst development. *J Geophys Res Biogeosci* 114:14.
- Vogel JS, Nelson DE, Southon JR. 1987. C-14 background levels in an accelerator mass-spectrometry system. *Radiocarbon* 29:323–33.
- Wickland KP, Striegl RG, Neff JC, Sachs T. 2006. Effects of permafrost melting on CO₂ and CH₄ exchange of a poorly drained black spruce lowland. *J Geophys Res Biogeosci* 111:13.
- Zimov SA, Davydov SP, Zimova GM, Davydova AI, Schuur EAG, Dutta K, Chapin FS. 2006. Permafrost carbon: stock and decomposability of a globally significant carbon pool. *Geophys Res Lett* 33:5.